LA-UR-82-325

Conf-810585--2

TITLE: THE JULY 29, 1977 MAGNETIC STORM: OBSERVATIONS AND MODELING OF ENERGETIC PARTICLES AT SYNCHRONOUS ORBIT

AUTHOR(S): D.N. Baker, T.A. Fritz and B. Wilken

LA-UR--82-325

DE82 008127

SUBMITTED TO: Proceedings of the IMS Assessment Symposium held at Goddard Space Flight Center 21-23 May 1981

University of California

LOS ALAMOS SCIENTIFIC LABORATORY

Post Office Box 1663 Los Alamos, New Mexico 87545

An Affirmative Action/Equal Opportunity Employer

The July 29, 1977 Magnetic Storm: Observations and Modeling of Energetic Particles at Synchronous Orbit

by

D. N. Baker

Los Alamos National Laboratory

Los Alamos, NM 87545

T. A. Fritz

Space Environment Laboratory, NOAA

Boulder, CO 80303

B. Wilken

Max-Planck-Institut fur Aeronomie

D-3411 Katlenburg-Lindau, F.R.G

Abstract

A brief description of the energetic particle studies carried out by Subgroup 6 of CDAW-2 is presented. Instrumentation onboard six spacecraft at (or near) geostationary orbit was used in the analysis. Timing of particle injection during the last, and largest, substorm on July 29, 1977 ($\sim$ 1200 UT) was investigated, as was the particle phase space density variation associated with this event. Energetic proton gradient anisotropies were also used to examine large-scale magnetospheric boundary motions. Finally, adiabatic modeling calculations were performed for the substorm event period, including effects of injection, convection, corotation, and particle drifts. We find substantial evidence to suggest storage of solar wind-derived energy in the magnetotail prior to the substorm and we find this stored energy to be suddenly released at substorm expansion onset. We also find particles at geostationary orbit to be newly accelerated during the substorm to energies $\gtrsim$ 1 MeV ($\mu \gtrsim$ 100 MeV/G) and modeling shows that these particles could have been convected (and injected) from beyond 10 R_E in the nightside magnetosphere.

Introduction

A primary thrust of Subgroup 6 of CDAW-2 was to study energetic particle variations on 29 July 1977. The types of studies carried out by subgroup 6 were basically four in number:

(1) Timing and morphology of particle injections;

(2) Variation of particle phase space densities;

(3) Measurement of boundary motions using ion (proton) gradient anisotropies; and

(4) Adiabatic modeling with increased particle flux (i.e., injection), convection, corotation, and drifts.

We here briefly discuss our findings derived from each of the above lines of inquiry. Our initial research efforts were concentrated on the 1200 UT substorm of 29 July. This was the last and largest (AE $\sim$ 1200 γ) of a series of substorms that occurred on 29 July following a worldwide SSC that occurred at 0027 UT [King et al., 1982; Wilken et al., 1982]. We concentrate here on measurements made at geostationary orbit (6.6 R_E) where six different spacecraft made extensive observations of the energetic particle behavior.

Observations

Figure 1 is a geocentric solar ecliptic projection of the positions of the primary, near-geostationary satellites used in the present study. The ATS-6 and 1977-007 spacecraft were located near one another at $\sim$ 0300 LT. ATS-6 had NOAA, Aerospace, and TRW energetic particle, UCLA magnetometer, and UNH plasma experiments on board, while 77-007 had Los Alamos energetic particle sensors on board. The Los Alamos-instrumented spacecraft 1976-059 at $\sim$0700 LT was bracketed by the GOES-1 and -2 satellites which carried NOAA energetic particle and magnetometer instruments. Finally, the European Space Agency satellite GEOS-1 ($1.3 \lesssim r \lesssim 7$ R_E) carried a complete complement of plasma and field measurement instruments and was located near apogee at $\sim$1300 LT.

General geomagnetic activity for July 28-30, 1977 has been discussed in the companion paper by Manka et al., [1982]. Particularly evident activity on these days included the storm sudden commencement (SSC), due to an interplanetary shock wave hitting the earth at 0027 UT on 29 July, and the rapid storm mainphase development thereafter. Also evident were the disturbed auroral zone conditions for the first part of 29 July and the large substorm (AL > 1000 γ) at $\sim$1200 UT.

Phase Space Density Variations

In the more detailed treatment of our CDAW results [Baker et al., 1982], we discussed pronounced flux increases associated with the 1200 UT substorm and have referred to these as injections. That is, we have presumed that the flux enhancements actually corresponded to 'fresh' particles transported to, or accelerated in the vicinity of, geostationary orbit. In order to confirm this supposition, we have evaluated the particle distribution functions at constant first adiabatic invariant. The advantage of studying the phase density at constant μ is that adiabatic (magnetic field) variations are removed. Thus true particle density increases or decreases are revealed and sources or sinks of particles can be identified. Figure 2 shows examples of the phase space density profiles calculated for electrons at μ = 1, 10, and 100 MeV/G. Evident features in the upper panel (77-007/ATS grouping) during the period 1130-1300 UT on 29 July were the following:

(1) Even with removal of adiabatic effects, the pronounced flux dropout between 1135 and 1155 UT persisted;

(2) The phase space densities at constant μ were identical before the dropout ($\sim$ 1130 UT) and after the dropout ($\sim$ 1155 UT);

(3) True phase space density increases were observed for all magnetic moments (energies) after 1200 UT.

The points above, therefore, demonstrate that in a broad sector near local midnight there was a large scale boundary motion which took the observing spacecraft into a low density region (i.e., across a spatial discontinuity). This thinning-like event preceded the substorm onset. Prior to the substorm onset the midnight-sector spacecraft also returned to a predropout density configuration for several minutes (1155-1200 UT); this, therefore, was not an injection event. At $\sim$ 1200 UT an injection of newly accelerated particles occurred for all magnetic moments.

The lower panel of Figure 2 shows the electron density variations at 0700 LT. Comparison of these results with electron flux variations at 0700 LT [Baker et al., 1982] shows that at this location virtually all flux variations before ~ 1205 UT were adiabatic. The phase space densities in this region of the magnetosphere showed essentially flat profiles prior to 1205, a density dip at ~ 1205, and energy-dispersed density increases after ~ 1206 UT, consistent with injection and drift from the west.

Gradient Anisotropy Information

By examining flux and phase space density variations (particularly at the 03 LT position), it is established that newly accelerated particles (up to several hundred MeV/G) appeared at synchronous orbit between ~ 1200 and 1210 UT on 29 July. The best available tool for examining the question of the general source region for the injected hot plasma and energetic particles is provided by ion gradient measurements. Because of their large gyroradii, 10-1000 keV protons can provide good information about density gradients that exist within a region of strong radial intensity variations or within an injected cloud of plasma and energetic particles.

Figure 3 shows the A_{EW} (east-west gradient anisotropy) values calculated from the 77-007 energetic proton data (E > 145 keV) combined with the average >145 keV proton flux. From these data, the following sequence of events is inferred. Between 1155 and ~1200, i.e., during the recovery from the flux dropout, A_{EW} was strongly positive. This suggests that the higher particle density was inside the spacecraft and below the spacecraft. Observations showed the field to be very taillike during this period, and thus our contention of a boundary motion during the dropout, with the high flux region moving earthward and equatorward, is borne out. As the fluxes recovered, the spacecraft was enveloped from inside and from below.

At 1200 UT, A_{EW} went strongly negative. This period corresponded to the first energetic particle and hot plasma injection into synchronous orbit. The character of A_{EW} showed that the injected particles came from outside the spacecraft location. The conclusion is, therefore, in this case that the injected particles arrived at 6.6 R_E from the outside and from above. This very likely means that these particles filled the high-latitude plasma sheet and that these filled field lines then collapsed inward over the spacecraft. After the leading edge of the particle injection passed over the spacecraft, A_{EW} went strongly positive (1202-1205 UT). This indicates that the highest density, after the injection, was generally inside 6.6 R_E.

A second particle injection occurred (cf. Figure 2) at ~ 1205 UT. Figure 3 shows again that these particles came from outside 6.6 R_E since A_{EW} was strongly negative. It is concluded with considerable certainty that the 1205 UT injection of energetic particles and hot plasma, as was also true for the 1200 UT case, came from outside of synchronous orbit.

Drift-Echo Timing Information

Proton drift-echo events can be used to infer times and locations of the 'centroids' of particle injections [Belian et al., 1978]. As illustrated by the detailed 10-s flux averages shown by Baker et al. [1982], the sharply-peaked pulses of drifting protons associated with the 1200 UT substorm show evidence of a triple structure in each pulse. These detailed flux values were used to determine carefully the time of the 'peak 1', 'peak 2' and 'peak 3' relative flux maxima for the 0.4-0.5, 0.5-0.6, 0.6-0.8, and 0.8-1.0 MeV channels at the 0700 and 0300 LT positions. Results for the several selected 76-059 and 77-007 energy channels are plotted here in Figure 4. In each panel we separately plot data for each of the peak 1 through peak 3 pulses. The parameter ϕ is equivalent to LT (in degrees) except that it runs clockwise from midnight (in the same sense as proton drifts) rather than counterclockwise. For each energy channel a least-squares fit through the data points is shown.

As seen by Figure 4, it is possible to arrive at an internally consistent interpretation of all of the high-energy proton data, at both 0700 LT and 0300 LT. This interpretation is that there were three high-energy proton injections centered in the post-midnight region and these injections each exhibited several echoes that were individually seen at both the 0700 and 0300 local times. The universal times of the injections inferred from Figure 4 are: peak 1 events, $\sim$ 1200 UT; peak 2 events, $\sim$ 1205 UT; and peak 3 events, $\sim$ 1208 UT.

Adiabatic Modeling Results

A major underlying theme of our analysis has been that substorm energetic particles are injected in the nightside magnetosphere and that these particles subsequently are trapped and drift to positions removed from the injection site. Much of the foregoing analysis has been carried out within this framework and , generally, supports such an interpretation. However, in order to model the injection and drift more quantitatively the time-dependent convection model of Smith et al. [1979] was used in CDAW-2.

Although this large-scale convection model has been quite successful in predicting the behavior of low-energy charged particles during storms [c.f. Smith et al., 1979], a goal of the CDAW-2 effort was to test the model for higher energy particle injections. To this end, protons with with μ = 1.0 keV/γ (100 MeV/G) and pitch angle = 90° were injected at a boundary of 10 R_E. For μ = 100MeV/G, the kinetic energy of the protons at L=6.6 would be about 100 keV.

It was found that the time-dependent convection model could produce trapped drift trajectories for the higher energy proton component ($\gtrsim$100 keV) [Baker et al., 1982]. The changes to the normal model in order to accomplish a large trapping ratio (such as changing the magnetic field gradient in the outer magnetosphere) appear quite consistent with spacecraft magnetometer observations and, thus, seem to provide reasonable physical improvements to the ordinary dipole-field model. In most cases, it was seen in the modeling that only high-energy protons injected near 0200-0300 LT were durably trapped. It is interesting that our proton drift-echo analyses also tend to show injection positions near 0200 LT for the observed proton pulses in this particular substorm case (c.f. Figure 4).

Discussion and Summary

In this paper we have summarized data from six satelites near geostationary orbit used to study an intense substorm period on July 29, 1977. These several spacecraft, well-distributed in local time, have given us a perspective on global substorm phenomenology not previously available. Several different analysis techniques (of which some are unique to energetic particles) were applied to the data sets and a self-consistent picture of the event period has emerged.

Based on the results presented here, some very firm conclusions regarding substorm phenomenology can be stated. First, there seems to be good evidence that the magnetosphere went through a period of substantial energy storage prior to the sudden energy release at $\sim$1200 UT [McPherron, 1970, Baker et al., 1978]. Our results also show that the injected substorm particles came from outside (and above) the spacecraft at $\sim$ 0300 LT. Adiabatic modeling showed that trapping can be simulated by convection of high-energy particles from beyond $10R_E$. Based on large numbers of other high-energy proton events observed at synchronous orbit and in the plasma sheet, Baker et al. [1979] argued in favor of the importance of induction electric fields. They showed from the timing and duration of energetic proton events that particles with energies of $\sim$ 1 MeV could not be produced by a small inward radial convection;

large impulsive acceleration must be responsible for their production. The high-energy proton results shown for this event are, therefore, consistent with the plasma sheet energization model presented by Baker et al.

In summary, it seems evident that the multiple-spacecraft observational approach used here is powerful one. Since the geostationary satellites that we have used in this CDAW study have acquired literally years of concurrent data, we look forward to many future joint studies of the effects of geomagnetic storms and substorms on magnetospheric energetic particle populations.

Acknowledgments

Work at Los Alamos was done under the auspices of the U.S. Department of Energy.

References

Baker, D. N., P. R. Higbie, E. W. Hones, Jr., and R. D. Belian, High-resolution energetic particle measurements at 6.6 R_E, 3, Low-energy electron anisotropies and short-term substorm predictions, J. Geophys. Res., 83, 4863, 1978.

Baker, D. N., R. D. Belian, P. R. Higbie, and E. W. Hones, Jr., High-energy magnetospheric protons and their dependence on geomagnetic and interplanetary conditions, J. Geophys. Res., 84, 7138, 1979.

Baker, D. N., T. A. Fritz, B. Wilken, P. R. Higbie, S. M. Kaye, M. G. Kivelson, T. E. Moore, W. Stüdemann, A. J. Masley, P. H. Smith and A. L. Vampola, Observation and modeling of energetic particles at synchronous orbit on July 19, 1977, J. Geophys. Res., in press, 1982.

Belian, R. D., D. N. Baker, P. R. Higbie, and E. W. Hones, Jr., High-resolution energetic particle measurements at 6.6 R_E, 2, High-energy proton drift echoes, J. Geophys. Res., 83, 4857, 1978.

King, J. H., R. P. Lepping, and J.D. Sullivan, On the complex state of the interplanetary medium on July 29, 1977, J. Geophys. Res., to be published, 1982.

Manka, R. H., T. A. Fritz, R. G. Johnson, R. A. Wolf, M. J. Teague, and J. I. Vette, The July 29, 1977 Magnetic storm: Introduction to the Coordinated Data Analysis Workshop, Proceedings of the IMS Assessment Symposium, 1982.

McPherron, R. L., Growth phase of magnetospheric substorms, J. Geophys. Res., 75, 5592, 1970.

Smith, P. H., N. K. Bewtra, and R. A. Hoffman, Motions of charged particles in the magnetosphere under the influence of a time-varying large scale convection electric field, Quantitative Modeling of Magnetospheric Processes, Geophys. Monograph, Vol. 21, (W.P. Olson, ed.), AGU, Washington, D.C. 1979.

Wilken, B., C. K. Goertz, D. N. Baker, P.R. Higbie, and T. A. Fritz, The SSC on July 29, 1977 and its propagation within the magnetosphere, J. Geophys. Res., in press, 1982.

Figure Captions

Fig. 1. Positions of the geostationary and near-geostationary (GEOS-1) spacecraft used in this study. The nominal magnetopause location in this solar ecliptic projection is also shown.

Fig. 2. Electron phase space density variations (computed as described in the text) for the 1200 UT substorm period. Densities at constant first invariant values (μ, as labelled) are plotted both for the 03 LT (top) and 07 LT (bottom) satellite positions.

Fig. 3. A comparison of the >145 keV proton flux (solid line) and the associated east-west gradient anisotropy (dotted line). Strong gradient anisotropies occur as new energetic particles are injected near synchronous orbit.

Fig. 4. Local time ('ϕ') versus UT plots for high-energy drift-echo pulses seen at S/C 1977-007 and 1976-059. As discussed in the text, the intersections of the manifolds of lines in each panel give an idea of the local time and universal time of the proton injection. The small inset polar plot in the central panel illustrates the S/C locations and the centroids of proton injection.

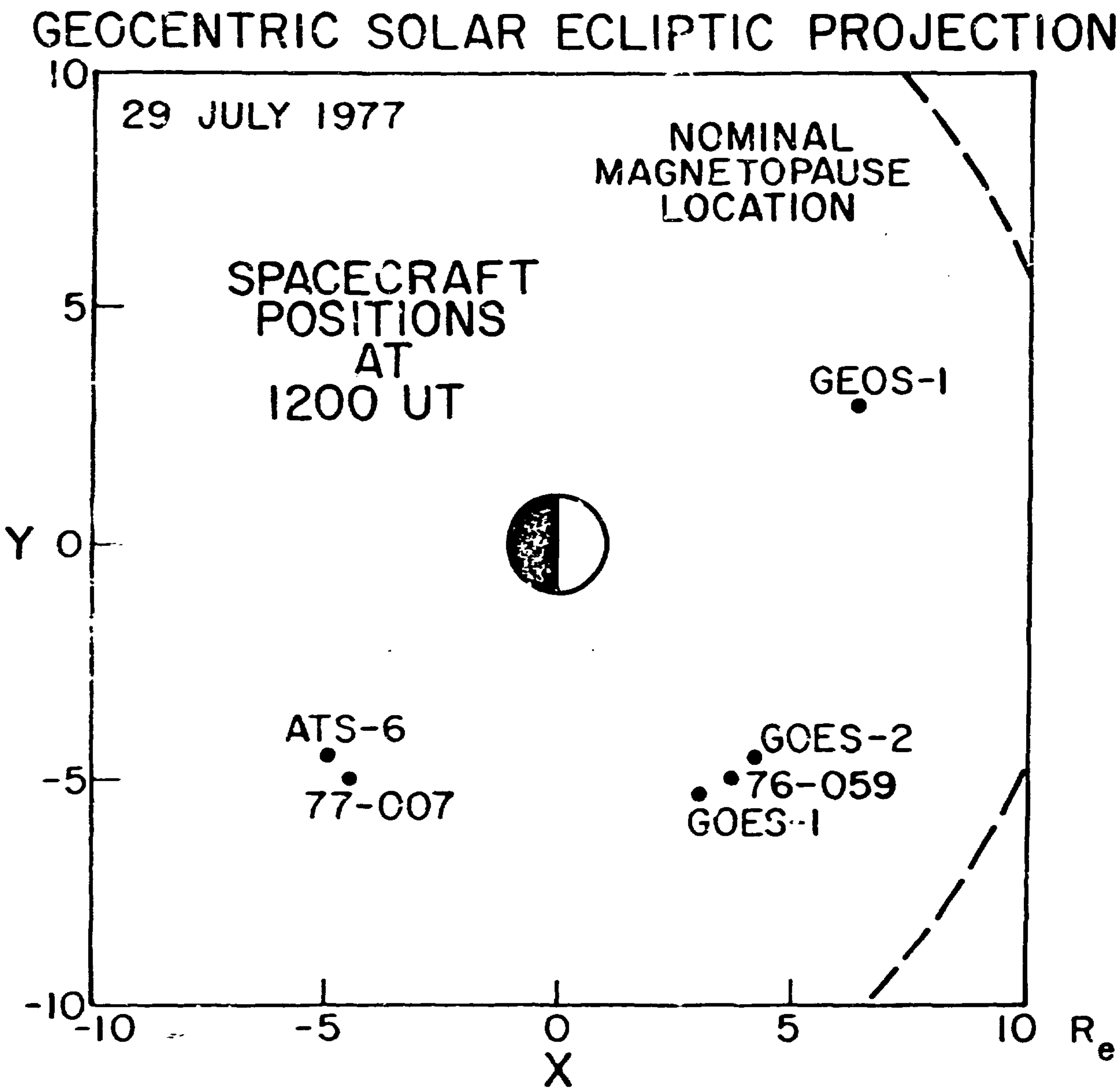
GEOCENTRIC SOLAR ECLIPTIC PROJECTION
29 JULY 1977
NOMINAL MAGNETOPAUSE LOCATION
SPACECRAFT POSITIONS AT 1200 UT
GEOS-1
ATS-6
77-007
GOES-2
76-059
GOES-1
Y
X
R_e
10
5
0
-5
-10
-10
-5
0
5
10

Fig. 1.

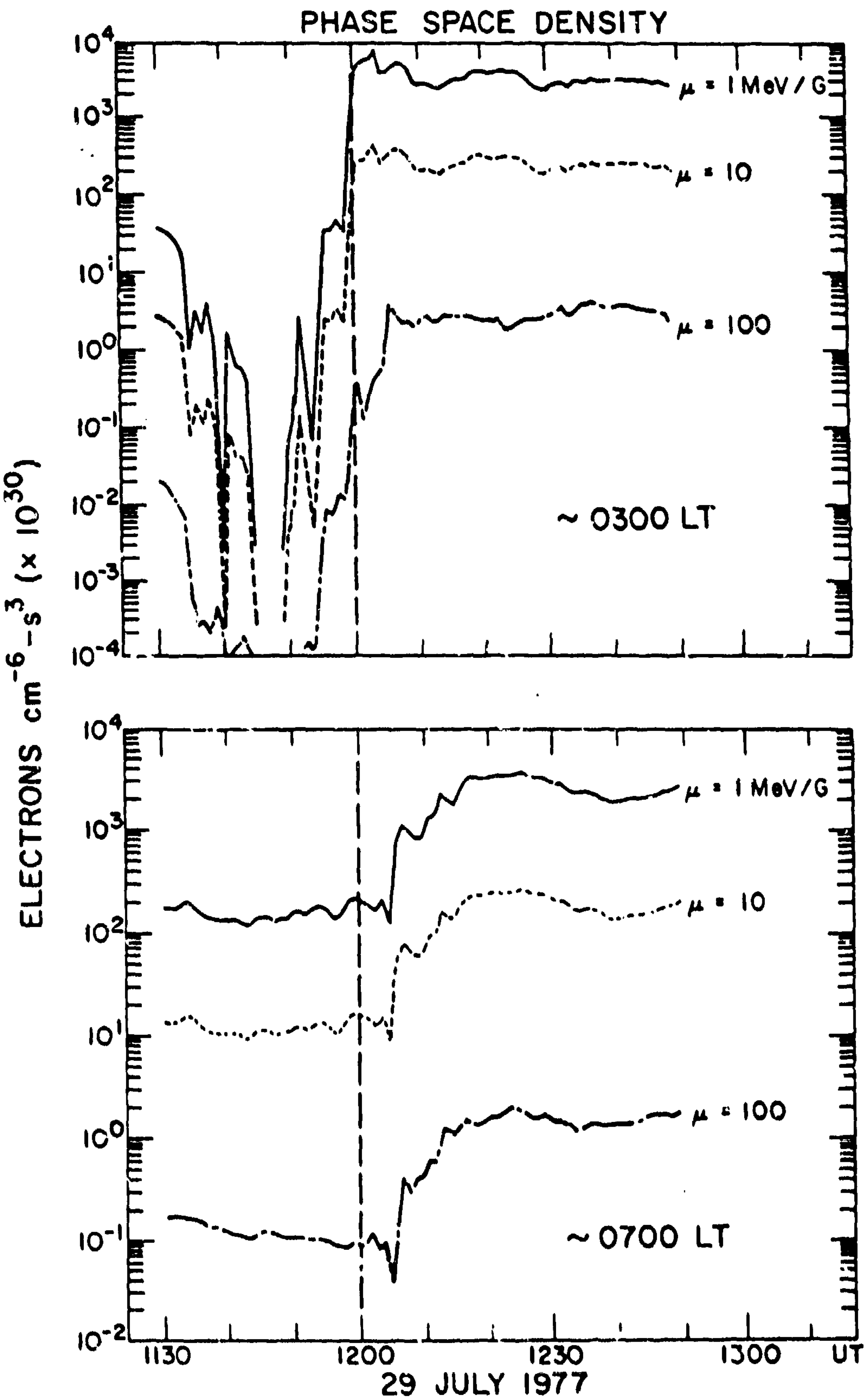

PHASE SPACE DENSITY
ELECTRONS cm^-6-s^3 (x 10^30)
μ = 1 MeV/G
μ = 10
μ = 100
~ 0300 LT
~ 0700 LT
1130
1200
1230
1300
UT
29 JULY 1977

Fig. 9.

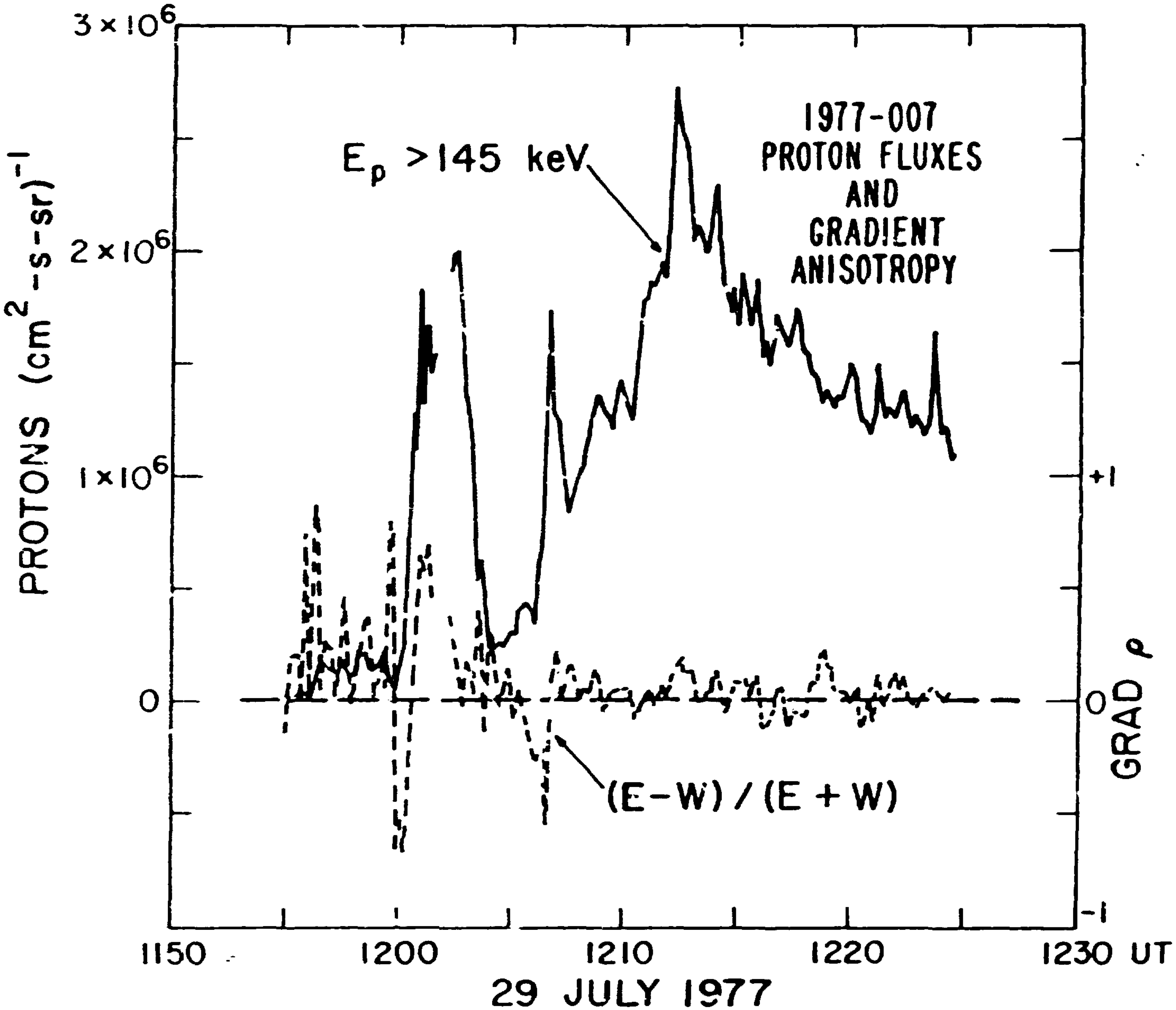

3×10^6
2×10^6
1×10^6
0
PROTONS (cm^2-s-sr)^-1
Ep >145 keV
1977-007
PROTON FLUXES
AND
GRADIENT
ANISOTROPY
(E-W)/(E+W)
+1
0
-1
GRAD ρ
1150
1200
1210
1220
1230 UT
29 JULY 1977

Fig. 3.

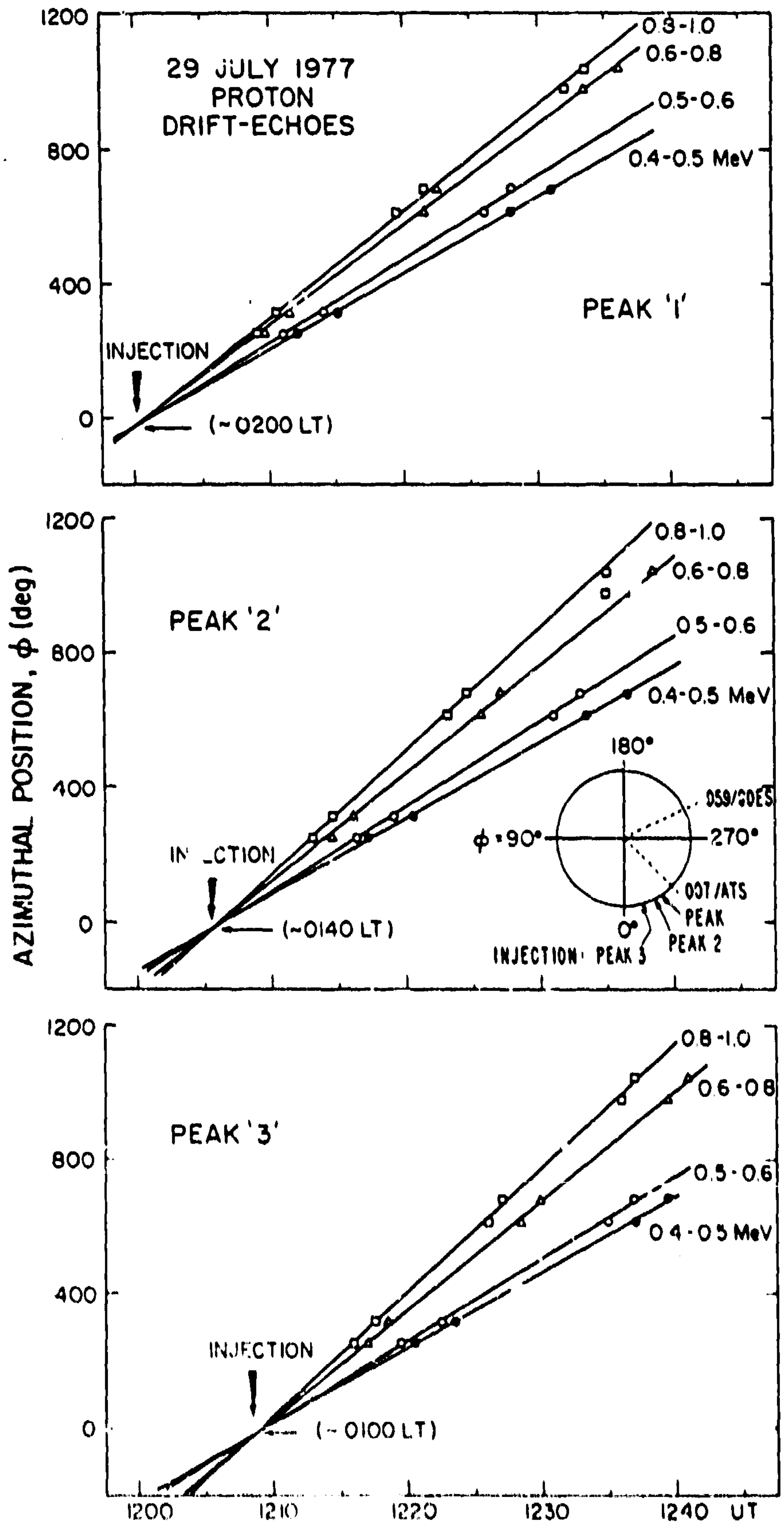
29 JULY 1977
PROTON
DRIFT-ECHOES
PEAK '1'
PEAK '2'
PEAK '3'
INJECTION
(~0200 LT)
(~0140 LT)
(~0100 LT)
0.8-1.0
0.6-0.8
0.5-0.6
0.4-0.5 MeV
AZIMUTHAL POSITION, ϕ (deg)
180°
ϕ = 90°
270°
0°
PEAK 2
PEAK 3
UT

Fig. 4.